Int. J. Electrochem. Sci., 15 **(2020)** 587 – 598, doi: 10.20964/2020.01.80

International Journal of
ELECTROCHEMICAL
SCIENCE
www.electrochemsci.org

Hydrothermal-assisted Synthesis of Li_2FeSiO_4/C Composites as Cathode Materials for Lithium-Ion Batteries

*Jing Li, Maolin Zhang**, *Tongtong Xue, Dongyan Zhang, Yangxi Yan, Zhimin Li**

School of Advanced Materials and Nanotechnology, Xidian University, Xi'an, 710071, China
*E-mail: mlzhang@xidian.edu.cn, zmli@mail.xidian.edu.cn

Received: 2 October 2019 / *Accepted:* 12 November 2019 / *Published:* 30 November 2019

Orthosilicate Li_2FeSiO_4 composites have recently attracted increasing attention as cathode materials of lithium-ion batteries (LIBs). However, diffusion-controlled kinetics of electrochemical processes limited their widespread applications. Carbon coatings are often deposited to improve the electrochemical performances of Li_2FeSiO_4 based cathode materials. In this work, hydrothermal assisted sol-gel method was used to prepare Li_2FeSiO_4/C electrode materials using sucrose as carbon source. Structures, morphologies, and electrochemical behaviors of obtained cathode materials were analyzed by X-ray diffraction, scanning electron microscopy, electrochemical impedance spectroscopy and galvanostatic charge-discharge measurements. The electrode material prepared using 2 wt% sucrose displayed the best initial discharge specific capacity reaching 174 mAh/g at 0.1 C and superior rate performance with 95.3% retention capacity. These improved electrochemical properties were attributed to well-developed hierarchical porous structure, enhanced Li-ion diffusion coefficient, and large exchange current of as-obtained electrode materials.

Keywords: Cathode materials; Li_2FeSiO_4/C; Electrochemical properties; Hierarchical porous structure

1. INTRODUCTION

Polyanionic cathodes have extensively been used in lithium-ion batteries (LIBs) due to their stable charge/discharge performance, excellent thermal stability, outstanding cycle properties, high safety, and environmental friendliness [1-2]. Typical polyanionic cathodes comprise $LiFePO_4$, widely used as energy storage material in electric vehicles. However, its limited theoretical capacity (170 mAh/g) hinders further development and applications [3-4].

As an alternative, orthosilicate Li_2FeSiO_4 has attracted increasing attention due to its high theoretical capacity, good safety and low-cost. Li_2FeSiO_4 could generate a theoretical capacity as high as 330 mAh/g, corresponding to 2 mol Li^+ per formula unit exchange [5]. Moreover, cathodes based on Li_2FeSiO_4 display superior stability due to strong Si-O bonding and frame structure, leading to better

cycle stability [6]. Besides, raw materials sources of Si and Fe are abundant and cheap, leading to low cost and environmental friendliness. Therefore, Li_2FeSiO_4 has intensively been investigated as cathode materials since its first synthesis by Nytén in 2005 [7].

However, the diffusion-controlled kinetics of Li_2FeSiO_4 electrochemical processes limited its widespread use [8]. The biggest problems rely on the poor activity of Li_2FeSiO_4 with low electronic conductivity (10^{-13} S/cm) and Li-ionic diffusion coefficient (10^{-17} cm^2/s), resulting in challenging Li-storages reversibility and stability [6, 9-10]. Furthermore, the intercalation and deintercalation of a second Li^+ ion require extremely high voltage (> 4.4 V), at which electrochemical decomposition of the electrolyte occurs [9]. Therefore, only one Li^+ is often deinterlaced [11], leading to low practical discharge specific capacities of Li_2FeSiO_4 when compared to the theoretical value [12]. Consequently, tremendous efforts have been devoted to further enhance the electrochemical properties of Li_2FeSiO_4 cathode materials.

Particle size and surface morphology are simple and effective ways to enhance the electrochemical properties of Li_2FeSiO_4 based cathode materials [13-14]. The reason for this has to do with migration time of Li^+, which is strongly related to diffusion length and diffusion coefficient (D_{Li}) of the active materials during intercalation and de-intercalation processes [15-17]. As a result, various kinds of nano-sized Li_2FeSiO_4 have been synthesized in the past years, including nanorods [18], shuttle-like particles [19], hollow spheres [20], fibrous structures [21], hierarchical pores structures [22] and ultrathin nanosheets [23]. These well-developed morphologies could stabilize the host structure and offer fast and consistent channels for the transport of lithium ions and electrons. This, in turn, would profoundly impact the electrochemical performances by increasing the reaction sites and surface wettability between the solid active particle and liquid electrolyte [13, 24-26].

Doping with foreign elements is another alternative and effective method to directly enhance the electrochemical properties of host Li_2FeSiO_4. Various cations might substitute the Fe site in Li_2FeSiO_4 by simple preparation routes. Cations, such as Mn [27-28], V [29], Sr [10], Mg [30], Sn [31], Ni [8], Ti [32], Ca [5], Co [33], Ce [34], Y [35] and Al [11] have so far been successfully doped into Li_2FeSiO_4 cathode materials. This method promoted the electrochemical properties of the resulting materials in terms of specific capacity, rate performance, and cycle performance. Another way for doping is by replacing the O site by anions, such as N [36-37], S [38], and F [39]. However, only a handful of research reports have been reported on this point.

The deposition of coatings on cathode materials is another method to improve the electrochemical performance of electrodes of LIBs. However, metal oxides (Al_2O_3 [40]), metal phosphates ($AlPO_4$ [41]) and fluorides are seldom used as coating materials on Li_2FeSiO_4 powders when compared to other cathode materials, such as $LiCoO_2$, NCM and NCA. Carbon coatings led to significant improvement of Li_2FeSiO_4 based cathode materials thanks to the excellent conductivity and chemical stability of carbon. Conductive nanocarbon materials, such as carbon nanoparticle, carbon nanotubes [42], graphene [43-44] and nano porous carbon [45] could favorably be compounded with Li_2FeSiO_4 host cathode materials due to their low cost, high electronic conductivity and favorable thermodynamic stability [6]. For instance, Guan prepared a novel MWNT@Li_2FeSiO_4 coaxial nanocable with high capacity of 180 mAh/g even at elevated rate of 1 C after 120 cycles [42]. Kumara synthesized Li_2FeSiO_4 nanocomposites with carbon nanofibers and reduced graphene oxide as conducting fillers [43]. The

resulting electrodes displayed enhanced electrochemical performances due to superior exchange current density and large contact areas between the electrolyte and cathode for efficient ion insertion and extraction.

On the other hand, various organic compounds have been widely used as carbon sources during the synthesis of Li_2FeSiO_4 as host materials, including glucose [46], tartaric acid [47], citric acid [48], oxalic acid [49], nonionic triblock copolymer P123 [50] and other newly introduced compounds [51]. These reagents are helpful in forming interconnected carbon frameworks and suppress crystal growth, leading to decreased pathways for rapid lithium-ion diffusion and enhanced electronic conductivity. This, in turn, would improve the electron transfer and Li^+ kinetics during the electrochemical processes [50]. Moreover, the reductive nature of organic compounds may prevent Fe^{2+} ions from oxidation into Fe^{3+}, leading to high purity Li_2FeSiO_4 products [49].

In this work, a hydrothermal assisted sol-gel method was employed to prepare Li_2FeSiO_4/C materials using sucrose as carbon source. X-ray diffraction (XRD), scanning electron microscopy (SEM), electrochemical impedance spectroscopy (EIS) and galvanostatic charge-discharge measurement were then used for in-depth characterization of the as-obtained Li_2FeSiO_4. The results showed Li_2FeSiO_4/C cathode materials with enhanced electrochemical properties thanks to interconnected carbon framework and reduced Li^+ diffusion coefficient.

2. EXPERIMENTAL

2.1 Preparation

Li_2FeSiO_4 based cathode materials with optimal electrochemical properties were firstly synthesized by the sol-gel method as previously reported [12]. The starting reagents $LiNO_3$, $Fe(NO_3)_3$, $Mn(NO_3)_2$, $C_6H_8O_7$, V_2O_5 and TEOS were all purchased from China National Pharmaceutical Group Co., Ltd. They were first mixed together in deionized water at pH=3 to form wet gel. Xerogel powder was then obtained after drying in an oven followed by grinding. Li_2FeSiO_4 based cathode material was obtained by heating at 650 °C for 10 h under nitrogen atmosphere to yield sample denoted as LSF.

Next, carbon-coated cathode powders were prepared by the hydrothermal route using sucrose as carbon source. The as-prepared LSF powder was mixed with sucrose in deionized water under vigorous stirring for 6 h. The mixture was then powered into the hydrothermal reactor and treated at 170 °C for 9 h. LFS/carbon compound powders were obtained after centrifugation and drying at 80 °C for 24 h. The powders obtained at LFS and sucrose mass ratios of 1:2%, 1:4% and 1:6% were denoted as LFS/C2, LFS/C4 and LFS/C6, respectively.

The as-prepared cathode powders were mixed with acetylene black (conductive agent) and PVDF (binder) at weight ratio of 80:10:10 through ball-milling for 10 min to produce cathode slurry, which was then pasted on Al foil to yield the positive electrodes of LIBs. Li metal, microporous polypropylene membrane (Celgard 2400) and $LiPF_6$ were used as anode, separator and electrolyte, respectively. Coin cells (CR-2016) were employed to test the electrochemical performances of the as-

obtained cathode materials. The fabrication process of CR-2016 cells was achieved according to previous literature [1-4].

2.2 Characterization

The phase structures of the obtained powders were analyzed by X-ray diffraction (XRD, D8 Advance, Bruker, Germany) over the 2θ range of 10-75° and step of 0.02°. Scanning electron microscopy (SEM, JSM-7500F, Jeol, Japan) was employed for morphology viewing. The charge and discharge properties of coin cells at various scanning rates were evaluated by multichannel galvanostatic system (CT2001A, Lanhe, China). The electrochemical impedance spectroscopy (EIS) of the coin cells were recorded on an electrochemistry workstation (CHI660E, Chinstruments, China) at amplitude of 5 mV and frequency from 10^{-2} - 10^{5} Hz.

3. RESULTS AND DISCUSSION

Figure 1 shows the XRD patterns of the as-synthesized Li_2FeSiO_4/C cathode materials. The diffraction peaks looked obviously sharp, indicating highly crystalline nature of the as-obtained compounds. Li_2FeSiO_4 could typically form three typical structures: orthorhombic structure (S.G. Pmn21), monoclinic structure (S.G. P21/n), and another orthorhombic structure with space group S.G. Pmnb.

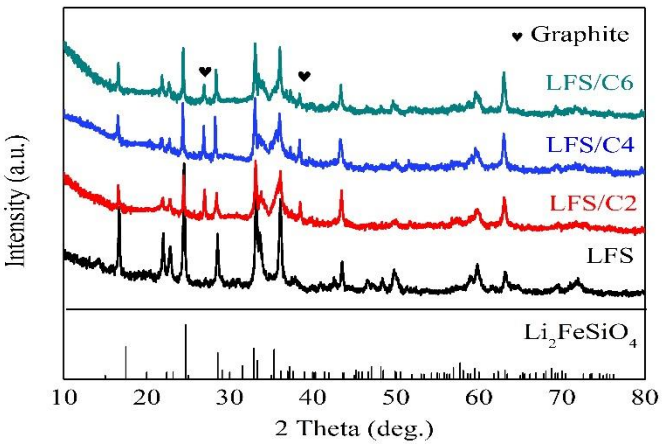

Figure 1. XRD patterns of as-prepared carbon-coated Li_2FeSiO_4 cathode materials.

These crystal phases could be obtained by hydrothermal method at about 400 °C, solid-state method at 700 °C and 900 °C, respectively [46, 49]. Here, the diffraction peaks matched well the monoclinic structure with space group of P21/n, consistent with reported literature [13, 46, 49]. However, graphitized carbon was observed on carbon-coated samples (LSF/C2, LSF/C4, and LSF/C6) due to large amounts of sucrose used as carbon source. Hence, sucrose was successfully carbonized.

The morphologies and microstructures of pure and carbon-coated LFS were confirmed by SEM. In figure 2, lamellar-like particles of LFS were obviously observed, consistent with our previous work [12]. However, the hierarchical porous structure was formed by carbonized sucrose as sucrose was introduced by the hydrothermal method in stainless steel tubes. The highly porous structure of LSF/C2 with wide pore size distribution from 100 to 800 nm was clearly displayed in figure 2 (B). Thus, LSF particles were successfully enveloped in interconnected carbon networks. This well-developed hierarchical porous structure may enhance the electrochemical properties of LSF/C2. Nevertheless, the hierarchical porous structure vanished as sucrose amount increased until the lamellar-like particles changed to spheroid particles.

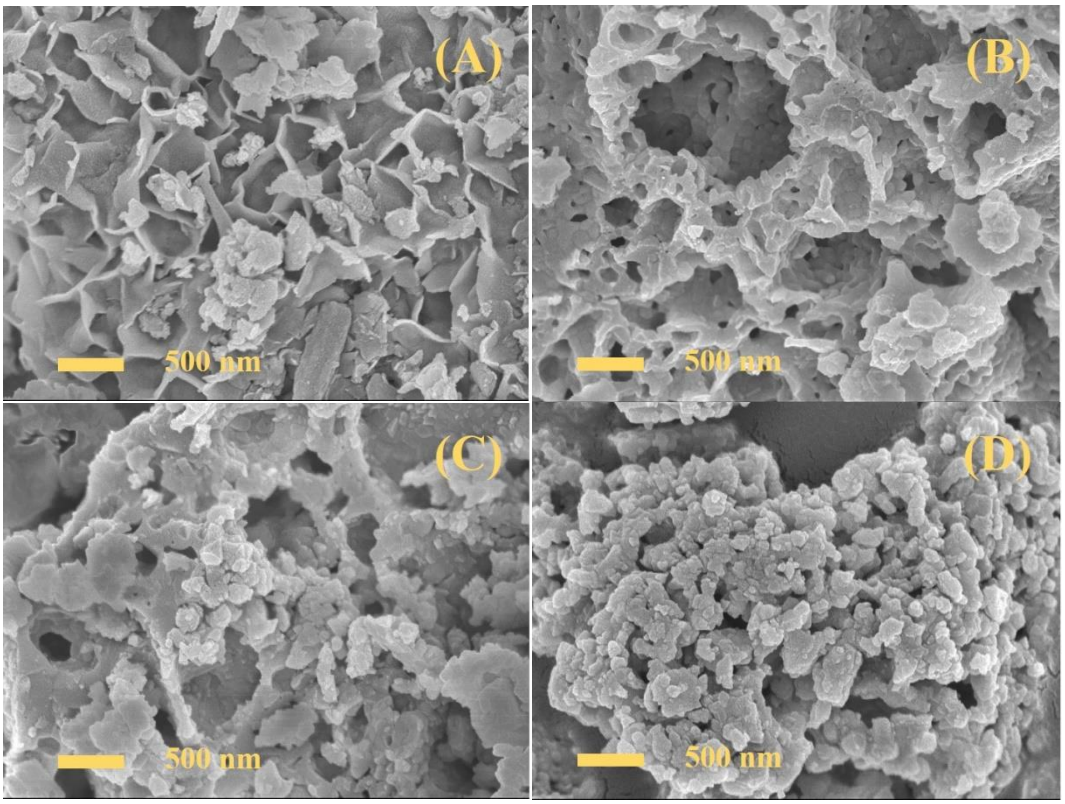

Figure 2. SEM images of various cathodes: LFS (A), LFS/C2 (B), LFS/C4 (C), and LFS/C6 (D).

To evaluate the initial capacities of various cathode materials, galvanostatic charge/discharge measurements were carried out in CR-2016 coin cells under 0.1 C rate (1 C = 166 mAh/g) from 1.5-4.7 V (figure 3 (A)). Despite the huge irreversible capacity, the carbon-coated electrodes showed obviously high charge specific capacities of 310, 234 and 210 mAh/g for LFS/C2, LFS/C4 and LFS/C6, respectively. Therefore, the initial coulombic efficiencies of carbon-coated electrodes were much lower than the uncoated electrodes (92.1%). This was mainly attributed to reaction between the active powders with electrolyte to form new solid electrolyte interface (SEI) film. Accordingly, the charge capacity fleetly decreased as cycling process continued (figure 3 (B)). However, the discharge capacities of the carbon-coated electrodes were estimated to 174, 149 and 157 mAh/g for LSF/C2, LSF/C4 and LSF/C6,

respectively. These values were higher than those obtained with uncoated LFS electrode (134 mAh/g).

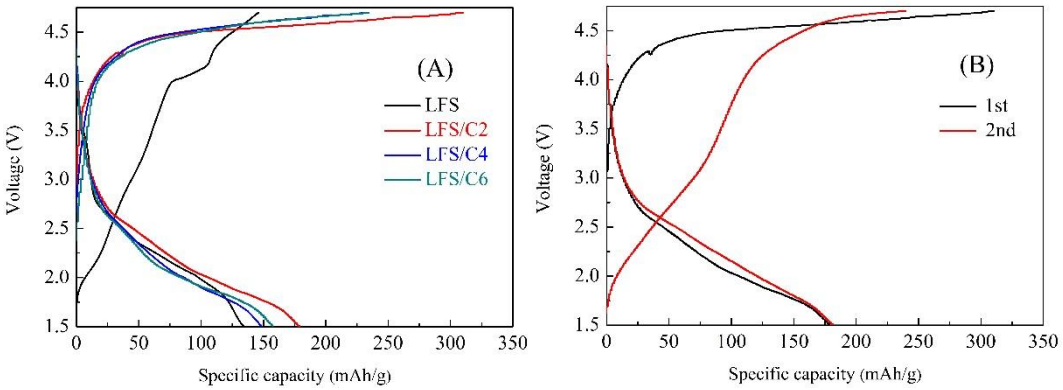

Figure 3. (A) Initial galvanostatic charge/discharge curves of various electrodes at 0.1 C between 1.5 and 4.7 V. (B) charge/discharge curves of LSF/C2 electrode at 0.1 C for the first and second cycles.

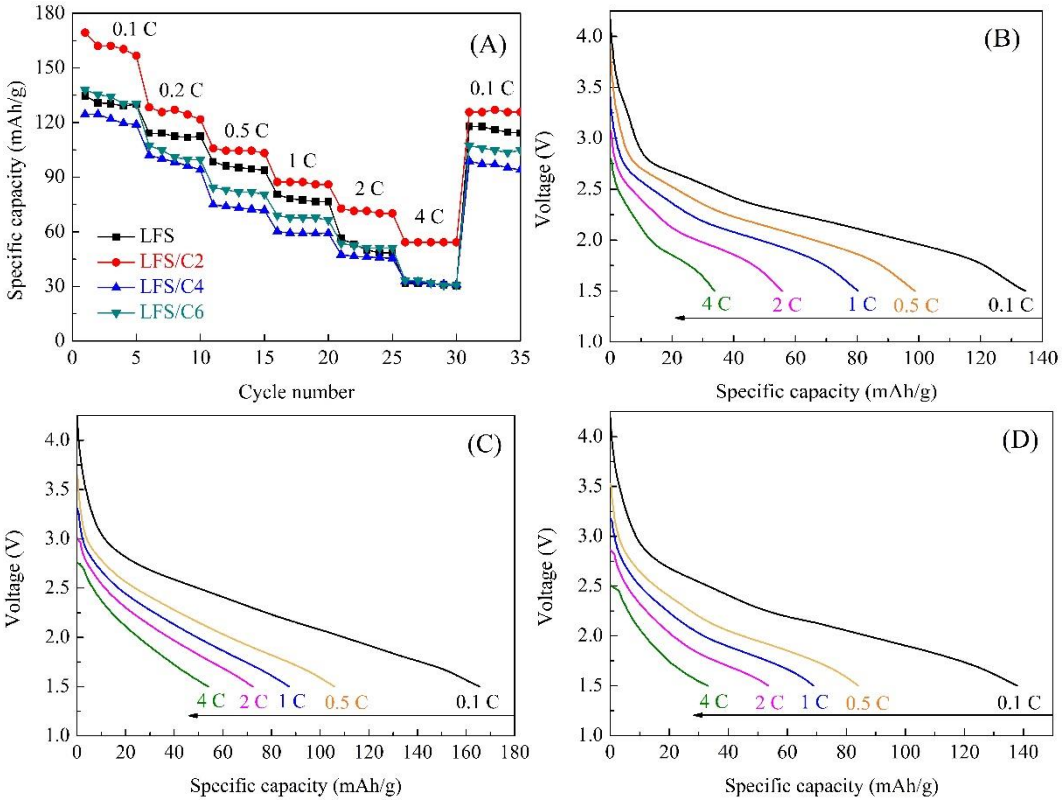

Figure 4. (A) Rate performances. Discharge behaviors of various cathode materials: LFS (B), LFS/C2 (C), and LFS/C6 (D) between 1.5 and 4.3 V using Li metal as anode.

Galvanostatic cycling was utilized to investigate the rate-dependent cycling performance of LFS and carbon-coated electrodes (LFS/C2, LFS/C4 and LFS/C6) at various charge/discharge rates from 0.1 to 4 C and then back to 0.1 C (5 cycles for each). LFS/C2 electrode showed the best rate cycling

performance with discharge capacities of 174, 129, 106, 88 and 73 mAh/g, at 0.1 C, 0.2 C, 0.5 C, 1 C and 2 C, respectively. Note that the discharge capacity of LFS/C2 electrode reached 55 mAh/g at 4 C, while the other electrodes displayed around 30 mAh/g. This excellent rate performance should be ascribed to the unique structure composed of hierarchical pores, providing fast transport channels for lithium ions. Also, interconnected carbon coating formed conductive networks, leading to enhanced conductivity (SEM images) [22].

Figure 5 displays the cyclic performance of pure and carbon-coated LFS cathodes at galvanostatic charge/discharge rate of 0.1 C and voltage from 1.5 to 4.3 V. The specific capacity of LFS cathode was only 134 mAh/g and tended to decline with retention around 78% after 100 cycles. The initial specific capacity of LFS/C2 electrode reached 174 mAh/g but rapidly decreased to 130 mAh/g in the first 20 cycles. Then the specific capacity of LFS/C2 electrode maintained stability with retention up to 95.3%, without significant capacity fading. These features can also be observed in discharge properties shown in figure 5 (C). Big skip distance was observed between the fist and 20th cycles while the discharge curves almost coincided between 20th and 100th cycles. The same phenomenon was observed for other carbon-coated electrodes. The discharge capacity quickly decreased within 20 cycles mainly due to formation of new solid electrolyte interface (SEI) film on carbon coated cathode materials. Unlike reported amorphous carbon coating films [45-46, 53], graphitized coating films required more cycling process to form stable SEI films. Therefore, no significant changes in retention capacities were observed for carbon-coated electrodes after 20 cycles.

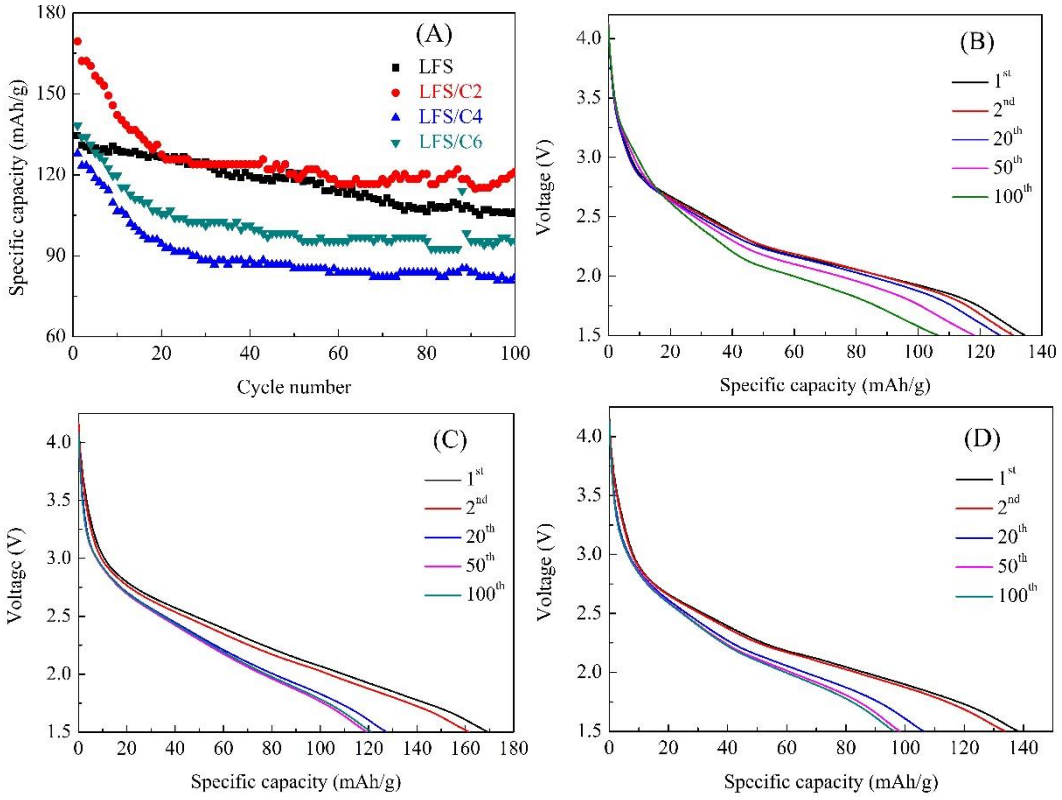

Figure 5. (A) Cycling performance of various electrodes. Discharge properties of LFS (B), LSF/C2 (C), and LSF/C6 at 0.1 C between 1.5 and 4.3 V using Li metal as anode.

Table 1. Electrochemical properties of Li_2FeSiO_4/C cathodes prepared by different methods and carbon sources.

Carbon Source	Method	Voltage range (V)	Initial capacity (mAh/g)	Capacity retention rate	Ref.
Sorbitan monolaurat	Sol-gel	1.5-4.8	187 at 0.1 C	95% after 50 cycles	[51]
Aitric acid	Sol-gel	1.5-4.8	182 at 0.1 C	32% after 50 cycles	[48]
Tartaric acid	Sol-gel	1.5-4.8	176 at 0.5 C	86% after 50 cycles	[47]
Oxalic acid	Two-step precipitation	1.5-4.3	171 at 0.1 C	92% after 50 cycles	[49]
Citric acid	Solid-state method	1.5-4.8	164 at 0.1C	95% after 10 cycles	[34]
Sucrose	Hydrothermal assisted sol-gel	1.5-4.3	174 at 0.1 C	95.3% after 100 cycles	This work

Table 1 shows the typical electrochemical properties of Li_2FeSiO_4/C cathode materials synthesized by different methods and carbon sources. It can be found that the carbon sources express great influence on the electrochemical properties of active materials. This is mainly attribute to the different coating appearances obtained by various carbon sources. It is obviously that the Li_2FeSiO_4/C cathode prepared with sucrose as carbon source displays high discharge capacity (174 mAh/g at 1.5-4.3 V) and good cycle stability. This excellent performance should be ascribed to the unique structure composed of hierarchical pores and the conductive networks formed by sucrose as carbon source.

To further discuss the electrochemical properties of the carbon-coated Li_2FeSiO_4 cathode powders, EIS measurements were carried out mainly to measure the lithium-ion diffusion and exchange current (figure 6). Obviously, the impedance profiles consisted of semicircle and inclined line, which can be divided into three regions: intercept at high frequencies, semicircle at medium frequencie, and sloping line at low frequencies (figure 6 (A)) [46, 49]. The intercept in Z′-axis represented R_e (ohmic resistance) of the electrolyte resistance between working and reference electrodes at high-frequencies. The semicircle at medium frequencies was assigned to charge transfer resistance (R_{ct}) between the electrolyte and electrode. At low frequencies, the inclined line was considered as Warburg impedance (Z_w), associated with lithium-ion diffusion in cathode active particles [49, 52-54]. The EIS data fitted by Z-View software are presented in figure 4 (B). Since the electrolyte was the same for all coin cells, Re values were similar for various electrodes and much lower than R_{ct}. However, R_{ct} values looked very different and estimated as 98, 91, 290 and 347 Ω for LFS, LFS/C2, LFS/C4 and LSF/C6 electrodes, respectively.

Therefore, suitable carbon coating would decrease charge-transfer resistance and enhance the electrochemical properties. Accordingly, the exchange current was calculated by Eq. (1) and the results are shown in figure 6 (D) [46, 49, 52-53].

$$i = \frac{RT}{nFR_{ct}} \quad (1)$$

where R, T, n and F are the gas constant, temperature, number of electrons per reaction species and Faraday constant, respectively.

To discuss the kinetics of Li^+ during intercalation/de-intercalation processes, the diffusion coefficients of Li^+ (D_{Li}) were calculated according to the literature [46, 49, 52-54],

$$D_{Li} = \frac{R^2T^2}{2A^2n^4F^4C^2\sigma^2} \quad (2)$$

where A is surface area of the electrode, C represents the molar concentration of Li ions during charge and discharge processes, σ is Warburg coefficient obtained from the slope of straight-line of Z′ and $\omega^{-1/2}$ [46, 49, 52-53].

$$Z' = R_e + R_{ct} + \sigma\omega^{-1/2} \quad (3)$$

where ω is the angular frequency at low frequencies.

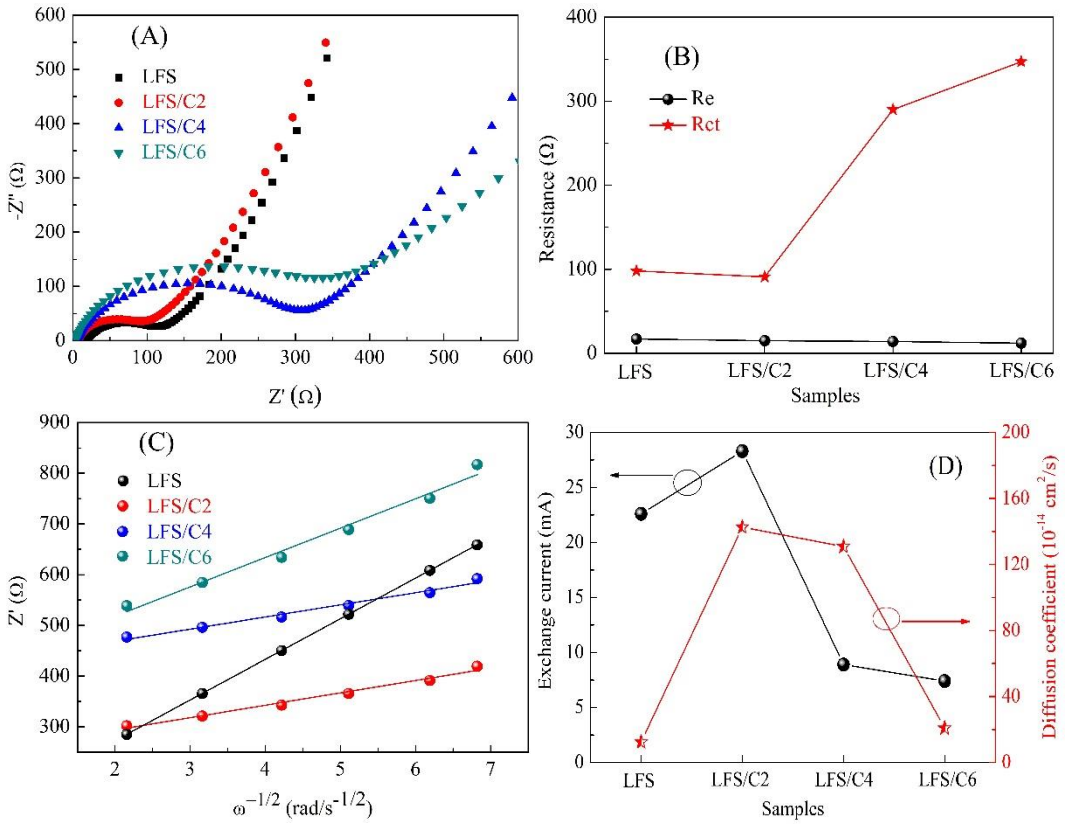

Figure 6. Electrochemical impedance spectra of various electrodes (A), ohmic resistance R_e and charge transfer resistance R_{ct} (B), relationship of Z′ and $\omega^{-1/2}$ in low-frequency range (C) and exchange current and lithium-ion diffusion coefficient of various electrodes (D).

The linear relationship between Z′ and $\omega^{-1/2}$ is shown in figure 6 (C). The diffusion coefficients of Li^+ for different electrodes can accordingly be obtained (figure 6 (D)). LFS/C2 electrode depicted the highest exchange current among all electrodes. It also exhibited an elevated lithium-ion diffusion

coefficient. LSF/C6 electrode illustrated the lower lithium-ion diffusion coefficient than LSF/C2 but still larger than that of pure Li_2FeSiO_4 (LFS). Therefore, carbon coating made by sucrose as carbon source through the hydrothermal process was effective for improving the kinetic properties of Li_2FeSiO_4. On the other hand, threshold for coating amount was recorded with LSF/C2 electrode expressing the highest exchange current and lithium-ion diffusion coefficient. This led to excellent electrochemical performance of LSF/C2 electrode. The suitable and uniform carbon coating of LSF/C2 electrode offered smaller hindrance for lithium ions diffusion since carbon coating network was intrinsically inert for lithium-ion diffusion [49].

4. CONCLUSIONS

Li_2FeSiO_4/C materials were successfully prepared by the hydrothermal assisted sol-gel method by using sucrose as carbon source. Hierarchical porous structure was formed through carbonization of suitable amount of sucrose (2 wt%) to form interconnected carbon networks. This, in turn, enhanced the Li-ion diffusion coefficient and increased the exchange current. LSF/C2 electrode depicted the best initial discharge specific capacity reaching 174 mAh/g at 0.1 C with superior rate performances and 95.3% capacity retention. In addition, the proposed method was facile, cheap and can easily be adapted to prepare other cathode materials.

ACKNOWLEDGEMENTS
This work was supported by the National Natural Science Foundation of China (No. 61701369 and 61974114); the Natural Science Basic Research Plan in Shaanxi Province of China (No. 2018JM6070 and 2018JM5060); the Fundamental Research Funds for the Central Universities (No. JB181407).

References

1. L. Yao, Y. Wang, J.H. Wu, M.W. Xiang, J.L. Li, B.Y. Wang, Y. Zhang, H. Wu and H. Liu, *Int. J. Electrochem. Sci.,* 12 (2017) 206-217.
2. Y.J. Zhang, Z.Y. Zhu, P. Dong, Z.P. Qiu, H.X. Liang and X. Li, *Acta Phys-Chimi. Sin.,* 33 (2017) 1085-1107.
3. Y. Gao, K. Xiong, H. Xu and B.F. Zhu, *Int. J. Electrochem. Sci.,* 14(2019) 3408-3417.
4. Z. Wang, D. Chen, Q.S. Ge, L.Q. Bai, L.S. Qin, G. Tang and Y.X. Huang, *Int. J. Electrochem. Sci.,* 14 (2019) 4611-4619.
5. L. Qu, M.T. Li, X.L. Tian, P. Liu, Y.K. Yi and B.L. Yang, *Chem. Phys.,* 503 (2018) 1-13.
6. K. Wang, W.J. Ren, J.L. Yang, R. Tan, Y.D. Liu and F. Pan, *Rsc Adv.,* 6 (2016) 47723-47729.
7. A. Nyte´n, A. Abouimrane, M. Armand, T. Gustafsson and J.O. Thomas, *Electrochem. Commun.,* 7 (2005) 156-160.
8. A.Y. Shenouda and M.M.S. Sanad, *J. Electrochem. Energy,* 14 (2017) 024501.
9. S. Thayumanasundaram, V.S. Rangasamy, J.W. Seo and J.P. Locquet, *Electrochim. Acta,* 258 (2017) 1044-1052.
10. L. Qu, M.T. Li, L.L. Bian, Q.Y. Du, M.L. Luo, B.L. Yang, L. Yang, S.H. Fang and Y. Liu, *J. Solid State Electr.,* 21 (2017) 3659-3673.
11. L. Li, E.S. Han, L.J. Dou, L.Z. Zhu, C. Mi, M. Li and J.H. Niu, *Solid State Ionics,* 325 (2018) 30-

42.
12. M.L. Zhang, H.C. Hu, J. Li, D.Y. Zhang, Y.X. Yan and Z.M. Li, *Int. J. Electrochem. Sci.,* 14 (2019) 11289-11299.
13. L.L. Yi, G. Wang, Y.S. Bai, M.H. Liu, X. Wang, M. Liu and X.Y. Wang, *J. Alloy. Compd.,* 721 (2017) 683-690.
14. J.F. Cui, C.X. Qing, Q.T. Zhang, C. Su, X.M. Wang, B.P. Yang and X.B. Huang, *Ionics,* 20 (2014) 23-28.
15. P.G. Bruce, B. Scrosati and J.M. Tarascon, *Angew. Chem. Int. Edit.*, 47 (2008) 2930-2946.
16. J.H. Liu, H.Y. Chen, J.N. Xie, Z.Q. Su, N.N. Wu and B.R. Wu, *J. Power Sources,* 251 (2014) 208-214.
17. A.S. Aricò, P. Bruce, B. Scrosati, J.M. Tarascon and W. Schalkwijk, *Nat. Mater.*, 4 (2005) 366-377.
18. J.L. Yang, L. Hu, J.X. Zheng, D.P. He, L.L. Tian, S.C. Mu and F. Pan, *J. Mater. Chem. A,* 3 (2015) 9601-9608.
19. J.L. Yang, X.C. Kang, D.P. He, T. Peng, L. Hu and S.C. Mu, *J. Power Sources,* 242 (2013) 171-178.
20. Y.M. Xu, W. Shen, A.L. Zhang, H.M. Liu and Z.F. Ma, *J. Mater. Chem. A,* 2 (2014) 12982-12990.
21. W.Y. Duan, T. Li, S.D. Li and K. Gao, *Mater. Lett.,* 250 (2019) 79-83.
22. X.J. Pu, G.J. Zhao, F. Ding, S.N. Cao and Z.X. Chen, *J. Solid State Electr.,* 22 (2018) 877-884.
23. D. Rangappa, K.D. Murukanahally, T. Tomai, A. Unemoto and I. Honma, *Nano Lett.,* 12 (2012) 1146-1151.
24. T.F. Yi, X.G. Hu, C.S. Dai and K. Gao, *J. Mater. Sci.*, 42 (2007) 3825-3830.
25. G. Wang, X.Y. Wang, L.L. Yi, R.Z. Yu, M.H. Liu and X.K. Yang, *J. Mater. Chem. A,* 4 (2016) 15929-15939.
26. G. Wang, X.Y. Wang, L.L. Yi, L.W. Wang, R.Z. Yu, M.H. Liu, D. Wang, Q.F. Ren and X.K. Yang, *RSC Adv.*, 6 (2016) 46325-46335.
27. H.J. Guo, X. Cao, X.Q. Li, L.M. Li, X.H. Li, Z.X. Wang, W.J. Peng and Q.H. Li, *Electrochim. Acta,* 55 (2010) 8036-8042.
28. P. Liu, Y. Gong, S. Nie, Q.S. Fu, L. Li, N.Q. Liu and J. Chen, *Ionics,* 25 (2019) 3611-3621.
29. Z. Zhang, X.Q. Liu, Y. Wu, H.Y. Zhao, B. Chen and W.Q. Xiong, *J. Electrochem. Soc.*, 162 (2015) 737-742.
30. A. Kumar, O.D. Jayakumar, Jagannath, P. Bashiri, G.A. Nazri, V.M. Naik and R. Naik, *Dalton T.,* 46 (2017) 12908-12915.
31. W. Sukkabot, *Mater. Chem. Phys.,* 229 (2019) 467-473.
32. S. Chakrabarti, A.K. Thakur and K. Biswas, *Electrochim. Acta,* 236 (2017) 288-296.
33. L.L. Zhang, S. Duan, X.L. Yang, G. Liang, Y.H. Huang, X.Z. Cao, J. Yang, M. Li, M.C. Croft, and C. Lewis, *J. Power Sources,* 274 (2015) 194-202.
34. L. Li, E.S. Han, H. Liu, C. Mi, Y.K. Shi and X. Yang, *Ionics,*25 (2019) 2965-2976.
35. H. Qiu, H. Yue, T. Zhang, Y. Ju, Y. Zhang, Z. Guo, C. Wang, G. Chen, Y. Wei and D. Zhang, *Electrochim. Acta,* 188 (2016) 636-644.
36. M. Armand and M.E.A. Dompablo, *J. Mater. Chem.*, 21 (2011) 10026-10034.
37. D. Zhang, T.T. Li, H.L. Qiu, Y.J. Wei, C.Z. Wang, G. Chen and H.J. Yue, *Chem. J. of Chinese U.*, 38 (2017) 1633-1638.
38. Y. Li, X. Cheng and Y. Zhang, *Electrochim. Acta,* 112 (2013) 670-677.
39. M. Armand, J.M. Tarascon and M.E.A. Dompablo, *Electrochem Commun,* 13 (2011) 1047-1050.
40. X.K. Huang, K. Chen and Y.Z. Liu, *Materi. Res. Express,* 1 (2019) 11-23.
41. H.L. Qiu, H.J. Yue, T. Zhang, T.T. Li, C.Z. Wang, G. Chen, Y.J. Wei and D. Zhang, *Electrochim. Acta,* 222 (2016) 1870-1877.
42. Y. Zhao, J.X. Li, N. Wang, C.X. Wu, Y.H. Ding and L.H. Guan, *J. Mater. Chem.,* 22 (2012) 18797-18800.

43. A. Kumara, T.P. Raoa, O.D. Jayakumarb, G.A. Nazria, V.M. Naikc and R. Naika, *Solid State Ionics*, 325 (2018) 43-47.
44. J.L. Yang, X.C. Kang, D.P. He, A.M. Zheng, M. Pan and S.C. Mu, *J. Mater. Chem. A*, 3 (2015) 16567-16573.
45. J.L. Yang, X.C. Kang, L. Hu, X. Gong and S.C. Mu, *J. Mater. Chem. A*, 2 (2014) 6870-6878.
46. J.L. Yang, X.C. Kang, L. Hu, X. Gong, D.P. He, T. Peng and S.C. Mu, *J. Alloy. Compd.*, 572 (2013) 158-162.
47. Z.M. Zheng, Y. Wang, A. Zhang, T.R. Zhang, F.Y. Cheng, Z.L. Tao and J. Chen, *J. Power Sources*, 198 (2012) 229-235.
48. T.T. Wu, C.Y. Lai and Q.J. Xu, *Mater. Lett.*, 186 (2017) 293-297.
49. B. Ren, Y.H. Xu, Y.L. Yan, R. Yang and J. Wang, *J. Alloy. Compd.*, 633 (2015) 456-462.
50. X.Z. Wu, X. Jiang, Q.S. Huo and Y.X. Zhang, *Electrochim. Acta*, 80 (2012) 50-55.
51. L. Qu, M.T. Li, P. Liu, X.L. Tian, Y.K. Yi and B.L. Yang, *Int. J. Electrochem.*, 13 (2018) 12311-12319.
52. A. Kumar, O.D. Jayakumar, V.M. Naik, G.A. Nazri and R. Naik, *Solid State Ionics*, 294 (2016) 15-20.
53. H.L. Qiu, K. Zhu, H.M. Li, T.T. Li, T. Zhang, H.J. Yue, Y.J. Wei, F. Du, C.Z. Wang, G. Chen and D. Zhang, *Carbon*, 87 (2015) 365-373.
54. L. Qu, D. Luo, S.H. Fang, Y. Liu, L. Yang, S. Hirano and C.C. Yang, *J. Power Sources*, 307 (2016) 69-76.